Progress In Electromagnetics Research B, Vol. 28, 111–128, 2011

A STRIP-MAP SAR COHERENT JAMMER STRUCTURE UTILIZING PERIODIC MODULATION TECHNOLOGY

Q. Liu, S. Xing, X. Wang, J. Dong, and D. Dai

School of Electronic Science and Engineering
National University of Defense Technology, Changsha 410073, China

Abstract—After being modulated by a periodic signal, the pulse compression result of the modulated LFM (Linear Frequency Modulation) may have many isolated and sharp peaks. According to this phenomenon, we developed a strip-map SAR (Synthetic Aperture Radar) jammer which modulated both the SAR's fast and slow time LFMs with periodic waveforms. This kind of jamming can forge isolated and bright points in the SAR image, and may confuse the SAR's image processing. The structure of this kind of jammer is simple and easy to be designed comparing to that of a traditional jammer utilizing the coherent jamming. Also it only needs much lower transmitted power than a noise jammer. Finally, the jamming experiences were conducted by utilizing a railway SAR, and the SAR imaging results showed the effectiveness of this kind of jamming.

1. INTRODUCTION

SAR (Synthetic Aperture Radar) is a powerful tool to discover targets under various kinds of conditions [1–4]. Both the SAR ECM (Electronic Counter Measures) and ECCM (Electronic Counter-Counter Measures) are old but still hot topics nowadays. According to the relationship between the jammings and the SAR transmitted signal, the SAR ECM technologies can be approximately divided into three kinds. If the jamming is within the same bandwidth of but incoherent to the SAR transmitted signal in the fast time, then it is usually called incoherent jamming, such as a noise jamming [5, 6]; If the jamming is coherent in the fast time (the range direction) but

Received 9 December 2010, Accepted 26 January 2011, Scheduled 2 February 2011
Corresponding author: Qingfu Liu (liu_675675@163.com).

incoherent in the slow time (the azimuth direction), then it is called partially coherent jamming, such as a repeater jamming [7, 8]; If the jamming is coherent both in the fast and slow time, then it is called coherent jamming, such as an active-decoy jamming [9]. Also, there are various kinds of SAR ECCM technologies. Most of them trace their genealogies back to the tradition radar technologies, e.g., the random waveform (such as the noise [10] and chaotic [11, 12] waveform) technology is now widely utilized in the agile-waveform SAR [13, 14], the space time adaptive processing technology [15] is utilized in the multi-channel SAR [16, 17], and the bistatic technology [18] is also utilized in the bistatic SAR [19]. After all, the SAR ECM and ECCM are a pair of paradoxes, and they are developed with the advancement of modern SAR theories and technologies. In this paper, only the topic of SAR ECM is focused and discussed by us.

An incoherent jamming can be easily generated by a jammer but needs high transmitted power, since it can not obtain the signal processing gains of the LFM (Linear Frequency Modulation) match filtering during the SAR imaging process both in the fast and slow time. This kind of jamming can be easily detected by SAR due to its large transmitted power, and can be cancelled through a number of ECCM technologies, e.g., wideband sidelobe-cancellation [16], spatial filtering [17] and adaptive beamforming [20]. A partially coherent jamming needs relatively lower transmitted power comparing to the incoherent jamming. In order to achieve a good coherency with the SAR transmitted signal in the fast time, this kind of jamming usually utilizes a DRFM (Digital Radio Frequency Memory) based jammer structure. But it can still be easily detected by SAR due to its relatively high transmitted power which makes it to be distinguishable from the real targets in the imaging scene, and may be cancelled by the ECCM technologies mentioned above. A coherent jamming needs the least transmitted power comparing to the other two kinds of jammings mentioned above and is hard to be detected by SAR. However, this kind of jamming usually needs to precisely estimate the slow time parameters of the SAR transmitted signal, e.g., the pulse repetition interval (PRI), the Doppler frequency, which are closely related to the SAR platform's movement and are difficult to be estimated in high precision by the jammer. So a jammer utilizing the coherent jamming is usually difficult to be designed and costly. In this paper, we proposed a coherent jamming with simple and easy to be designed jammer structure. The principles of this kind of jamming and the corresponding experiment results are shown as follows.

2. THE LFM'S PULSE COMPRESSION WITH COHERENT MODULATION

As we known, a classical SAR system utilizes the two-dimension LFM pulse compressions to reconstruct a 2-D image. The jamming received by SAR is indeed subject to the same signal processing steps of the real targets return, and its influence on the SAR imaging result can be interpreted as the output of the 2-D LFM match filtering with itself as the input. In order to better understand the principles of the jamming proposed in this paper, some basic properties of LFM and its pulse compression are given in the following part.

2.1. LFM and Its Pulse Compression

A LFM after I/Q demodulation and with unit amplitude can be written as

$$s(t) = \text{rect}[t/T] \exp\left\{j\pi K t^2\right\} \tag{1}$$

where

$$\text{rect}[t/T] = \begin{cases} 1 & |t| \le T/2 \\ 0 & \text{otherwise} \end{cases} \tag{2}$$

$j^2 = -1$, T is LFM's pulse width, K is chirp rate, and $B = |K|T$ is bandwidth. And the auto-correlation of $s(t)$ is

$$R_s(\tau) = \text{rect}\left[\frac{\tau}{2T}\right] \frac{\sin[\pi K\tau(T - |\tau|)]}{\pi K\tau} \triangleq R(\tau; T, K) \tag{3}$$

When $\tau = 0$, $|R_s(\tau)|$ has its maximum value $|R_s(0)| = T$. Also, (3) can be deemed as the pulse compression of the radar return which contains only one isolated and point-like scatterer with unit amplitude.

2.2. The Pulse Compression of a Complex Single Tone Modulated LFM

If $s(t)$ in (1) is modulated by a complex single tone $\exp\{j2\pi f_m t\}$, it becomes

$$\tilde{s}(t) = s(t) \exp\left\{j2\pi\tilde{f}t\right\} = \text{rect}[t/T] \exp\left\{j\pi\left(2\tilde{f}t + Kt^2\right)\right\} \tag{4}$$

And the pulse compression of $\tilde{s}(t)$, namely, the cross-correlation between $\tilde{s}(t)$ and $s(t)$ is:

$$\begin{aligned} & R_{\tilde{s}s}(\tau) \\ = & \int \tilde{s}(t) s^*(t+\tau)\, dt \\ = & \operatorname{rect}\left[\frac{\tau}{2T}\right] \frac{1}{\pi K\left(\tau-\frac{\tilde{f}}{K}\right)} \sin\left[\pi K\left(\tau-\frac{\tilde{f}}{K}\right)(T-|\tau|)\right] \exp\left\{-j\pi\tilde{f}\tau\right\} \\ \triangleq & \tilde{R}\left(\tau; T, K, \tilde{f}\right) \end{aligned} \tag{5}$$

When $\tau = \tilde{f}/K$, $|\tilde{R}(\tau; T, K, \tilde{f})|$ has its maximum value $|\tilde{R}(\tilde{f}/K; T, K, \tilde{f})| = T - |\tilde{f}/K|$. From (3) and (5), it can be seen that $|\tilde{R}(\tau; T, K, \tilde{f})|$'s peak is shifted by the amount of $\tilde{f}/K$ from the $\tau = 0$ position, and when $|\tilde{f}| \le |K|T = B$, the ratio between the maximum values of $|\tilde{R}(\tau; T, K, \tilde{f})|$ and that of $R(\tau; T, K)$ is

$$\eta\left(\tilde{f}\right) = \frac{\max\limits_{\tau}\left|\tilde{R}\left(\tau; T, K, \tilde{f}\right)\right|}{\max\limits_{\tau}\left|R(\tau; T, K)\right|} = \frac{T - \left|\tilde{f}\right| K^{-1}}{T} \tag{6}$$

So when the absolute value of the tone frequency is smaller than that of the LFM's bandwidth, the pulse compression result of a complex single tone modulated LFM will has a smaller and shifted peak. Otherwise, the pulse compression will have zero output.

2.3. The Pulse Compression of a Single Tone Modulated LFM

If $s(t)$ is modulated by a single tone $\sin\{2\pi f_m t\}$, then it becomes

$$\hat{s}(t) = s(t)\sin\{2\pi f_m t\} = \frac{1}{j2}\left[s(t)\exp\{2\pi f_m t\} - s(t)\exp\{-2\pi f_m t\}\right] \tag{7}$$

where $\hat{s}(t)$ is the combination of two complex single tone modulated LFMs with two opposite modulation frequencies. So $\hat{s}(t)$'s pulse compression has two peaks with the same amplitude and being shifted by the amount of f_m/K and $-f_m/K$ from the $\tau = 0$ position, respectively. That is

$$R_{\hat{s}s}(\tau) = \int \hat{s}(t) s^*(t+\tau) dt = \frac{1}{j2}\left[\tilde{R}(\tau; T, K, f_m) - \tilde{R}(\tau; T, K, -f_m)\right] \tag{8}$$

2.4. The Pulse Compression of a Periodic Waveform Modulated LFM

For a periodic waveform, it can be denoted as

$$q(t) = q_0(t) \qquad mT_q \le t < (m+1)T_q \tag{9}$$

where T_q is the period of $q(t)$, $q_0(t) = 0$ for $t < 0$ or $t > T_q$, $m = 0, \pm 1, \pm 2, \pm 3, \ldots$, and another more concise form of $q(t)$ can be written as

$$q(t) = q_0(t) \otimes_t \delta_{T_q}(t) \tag{10}$$

where

$$\delta_{T_q}(t) = \sum_{m=-\infty}^{+\infty} \delta(t - mT_q) \tag{11}$$

is a periodic Dirac function. And its Fourier transform is

$$\delta_{f_q}(f) = f_q \sum_{m=-\infty}^{+\infty} \delta(f - mf_q) \tag{12}$$

where $f_q = 1/T_q$ is the period of $\delta_{f_q}(f)$ and also the frequency of $\delta_{T_q}(t)$. Since convolution in the time domain is equivalent to multiplication in the frequency domain, the Fourier transform of $q(t)$ in (10) can be written as

$$Q(f) = Q_0(f) \cdot \delta_{f_q}(f) = f_q \sum_{m=-\infty}^{+\infty} Q_0(mf_q) \cdot \delta(f - mf_q) \tag{13}$$

That is

$$q_0(t) \otimes_t \delta_{T_q}(t) \quad \leftrightarrow \quad f_q \sum_{m=-\infty}^{+\infty} Q_0(mf_q) \cdot \delta(f - mf_q) \tag{14}$$

If a LFM signal $s(t)$ is modulated by $q(t)$, then it becomes

$$\tilde{s}_M(t) = q(t)\, s(t) = \left[q_0(t) \otimes_t \delta_{T_q}(t)\right] \cdot s(t) \tag{15}$$

So $\tilde{s}_M(t)$'s Fourier transform is

$$\begin{aligned} \tilde{S}_M(f) &= Q(f) \otimes_f S(f) \\ &= \left[f_q \sum_{m=-\infty}^{+\infty} Q_0(mf_q)\, \delta(f - mf_q)\right] \otimes_f S(f) \\ &= f_q \sum_{m=-\infty}^{+\infty} Q_0(mf_q)\, S(f - mf_q) \end{aligned} \tag{16}$$

After all, another form of $\tilde{s}_M(t)$ in (15) can be gotten from the inverse Fourier transform of $\tilde{S}_M(f)$ in (16)

$$\tilde{s}_M(t) = \sum_{m=-\infty}^{+\infty} f_q Q_0(mf_q) \left[s(t) \exp\{j2\pi m f_q t\} \right] \tag{17}$$

It can seen from (17) that, a periodic waveform modulated LFM is equivalent to a multi-tone modulated LFM. Because the LFM pulse compression is linear, the pulse compression of $\tilde{s}(t)$ can be deemed as the summation of each single tone modulated LFM' pulse compression. Combining (4), (5) and (17), the pulse compression of $\tilde{s}(t)$ can be written as

$$R_{\tilde{s}_M s}(\tau) = \sum_{m=-\infty}^{+\infty} f_q Q_0(mf_q) \tilde{R}(\tau; T, K, mf_q) \tag{18}$$

where $\tilde{R}(\tau; T, mf_q, K)$ is the function defined in (5). So the interval between the two adjacent peaks is

$$\delta_{\tilde{s}_M} = f_q / |K| \tag{19}$$

And the maximum value of the mth peak is

$$\Lambda_{\tilde{s}_M} = f_q Q_0(mf_q)(T - |mf_q/K|) \tag{20}$$

3. AN APPROXIMATION OF THE STRIP-MAP SAR'S TWO DIMENSION PULSE COMPRESSIONS

A strip-map SAR uses two dimension pulse compressions both in range and azimuth directions to reconstruct a image. After the range cell migration correction (RCMC) during the imaging process, both directions' pulse compressions can be approximately deemed as independent of each other [21], and this will greatly facilitate our analysis.

During the imaging process, the complex baseband reference signal for pulse compression in fast time can be written as

$$s_r(t_r) = \text{rect}\left[\frac{t_r}{T_r}\right] \cdot \exp\left\{j\pi K_r t_r^2\right\} \tag{21}$$

where the subscript "r" denotes the fast time(in range direction), t_r is the fast time; T_r is the pulse width; K_r is the chirp rate. $B_r = |K_r| T_r$ is the bandwidth.

Also, the reference signal for pulse compression in slow time can be approximated as

$$s_a(t_a) \approx \text{rect}\left[\frac{t_a}{T_{\text{syn}}}\right] \cdot \exp\left\{j\pi K_a t_a^2\right\} \tag{22}$$

where the subscript "a" denotes the slow time(azimuth direction), t_a is the slow time; T_{syn} is the synthetic aperture time; $K_a = 2v_a^2/(\lambda r_0)$ is the Doppler chirp rate, and v_a is SAR platform velocity; λ is the carrier wavelength, r_0 is the minimal slant range between SAR and the jammer. $B_a = |K_a|T_{\text{syn}}$ is the Doppler bandwidth.

Moreover, $s_r(t_r)$ in (21) and $s_a(t_a)$ in (22) can both be deemed as the jammer's received LFM signals from SAR in range and azimuth directions, respectively. And both $s_r(t_r)$ and $s_a(t_a)$ are with unit amplitude.

4. THE COHERENT JAMMING WITH PERIODIC MODULATION

4.1. The Frequency-shift Jamming

This kind of jamming can be described as follows. During each PRI in fast time, a DRFM based jammer receives the SAR transmitted LFM, modulates its received LFM with a single tone waveform, then transmits the modulated LFM back to SAR. If the tone frequency f_{fixed} remains the same during all the pulses within a synthetic aperture time, then the jamming is called fixed frequency-shift jamming. If the tone frequency starts with a initial value f_{init}, changes from pulse to pulse with a step of f_{step}, and rebounds to the first pulse's frequency f_{init} after each L_0 pulses, then this jamming is called step frequency-shift jamming. Also, there are other methods to change the tone frequency to generate other forms of frequency-shift jamming. Here we do not list them in the same detail because they can generally be analyzed in a similar way. For the fixed frequency-shifting jamming, the peak of the pulse compression in range direction will be shifted by the amount of f_{fixed}/K_r and the peak's maximum value will be reduced to $(T_r - |f_{fixed}|K_r)T_r^{-1}$ times of the its original value, namely, the peak's maximum value of the pulse compression without any modulation. Since the jamming induced points is shifted by the same amount of displacement in the range direction and will be in the same azimuth position after RCMC, the fixed frequency-shift jamming's pulse compression in azimuth direction will not be affected. For step frequency-shifting jamming, the displacements of the pulse compression's peaks in range direction are different from each other over different azimuth samplings, so the azimuth pulse compression may be affected by its insufficient sampling, i.e., over different PRIs, only the peaks within the same range bin can be coherently combined by the azimuth pulse compression. And this will cause the effect of insufficient sampling in slow time.

After l_0 steps of the step frequency-shift, the interval between the 1st and the (l_0+1)th peak of pulse compression in range direction is $l_0 f_{\text{step}}/K_r$. If l_0 satisfies the following condition

$$\begin{cases} l_0 > \dfrac{|K_r|B_r^{-1}}{\left|f_{\text{step}}\right|} = \dfrac{T_r^{-1}}{\left|f_{\text{step}}\right|} \\ l_0 - 1 \le \dfrac{T_r^{-1}}{\left|f_{\text{step}}\right|} \end{cases} \tag{23}$$

Then the interval will not exceed a range bin, since B_r^{-1} in (23) governs the slant range resolution. But the interval between the 1st and the (l_0+1)th peak will exceed a range bin, implying that their azimuth samplings can not be combined in slow time for azimuth pulse compression. So the azimuth insufficient sampling in slow time caused by the step frequency-shift in fast time can be written as

$$u_a(t_a) = \text{rect}\left(\frac{t_a}{l_0 T_a}\right) \otimes_{t_a} \sum_{m=-\infty}^{+\infty} \delta(t_a - mL_0T_a) \tag{24}$$

Notice that $u_a(t_a)$ is periodic, and the azimuth insufficient sampling can also be deemed as a periodic modulation in slow time. Multiplying $u_a(t_a)$ in (24) with $s_a(t_a)$ in (22) (deemed as the jammer's received LFM in slow time with unit amplitude), the jamming in slow time can be written as

$$\begin{aligned} \tilde{s}_{Ma}(t_a) &= u_a(t_a) \cdot s_a(t_a) \\ &\approx \left\{ \underbrace{\left[\text{rect}\left(\frac{t_a}{l_0 T_a}\right)\right]}_{u_0(t_a)} \otimes_{t_a} \underbrace{\sum_{m=-\infty}^{+\infty} \delta(t_a - mL_0T_a)}_{\delta_{L_0T_a}(t_a)} \right\} \\ &\quad \cdot \left\{ \underbrace{\text{rect}\left[\frac{t_a}{T_{syn}}\right] \exp\left\{j\pi K_a t_a^2\right\}}_{s_a(t_a)} \right\} \end{aligned} \tag{25}$$

Comparing (15) and (25), it can be found that $u_a(t_a)$, $\delta_{L_0T_a}(t_a)$, and $s_a(t_a)$ in (25) are the analogies to $q_0(t)$, $\delta_{T_q}(t)$, and $s(t)$ in (15), respectively. According to (17), (18), and (25), $\tilde{s}_{Ma}(t_a)$'s pulse compression can also be written as

$$R_{\tilde{s}_{Ma}s_a}(\tau) = \sum_{m=-\infty}^{+\infty} L_0^{-1} F_a U_a(mL_0^{-1}F_a) \tilde{R}(\tau; T_{\text{syn}}, K_a, mL_0^{-1}F_a) \tag{26}$$

where

$$\begin{aligned} U_a\left(mL_0^{-1}F_a\right) &= j\mathcal{T}\left\{u_a\left(t_a\right)\right\}\Big|_{f_a=mL_0^{-1}F_a} \\ &= l_0T_a\frac{\sin\left(\pi l_0T_af_a\right)}{\pi l_0T_af_a}\Big|_{f_a=mL_0^{-1}F_a} \\ &= l_0T_a\frac{\sin\left(\pi l_0L_0^{-1}m\right)}{\pi l_0L_0^{-1}m} \end{aligned} \tag{27}$$

So the interval between the two adjacent peaks is

$$\delta_{\tilde{s}_{Ma}} = L_0^{-1}F_a/\left|K_a\right| \tag{28}$$

And the maximum value of the mth peak is

$$\Lambda_{\tilde{s}_{Ma}} = L_0^{-1}F_aU_a\left(mL_0^{-1}F_a\right)\left(T_{\text{syn}} - \left|mL_0^{-1}F_a/K_a\right|\right) \tag{29}$$

So the step frequency-shift jamming not only shifts the peak of the pulse compression in range direction, but also defocuses the pulse compression in azimuth direction by introducing a period modulation in slow time. From (28) and (29), it can be seen that, as L_0 increases, i.e., the period of the step frequency-shift jamming increases, the interval between two adjacent peaks and the maximum value of each peak decrease, but the number of the peaks increases. Typically, if $l_0 = L_0$, i.e., the slow time modulation introduced by the step frequency-shift jamming is negligible, then (27) can be reduced to

$$\begin{aligned} U_a\left(mL_0^{-1}F_a\right) &= L_0T_a\frac{\sin\left(m\pi\right)}{m\pi} \\ &= \begin{cases} L_0T_a & \text{if} \quad m=0 \\ 0 & \text{otherwise} \end{cases} \end{aligned} \tag{30}$$

And $R_{\tilde{s}_{Ma}s_a}(\tau)$ in (26) can be reduced to

$$R_{\tilde{s}_{Ma}s_a}\left(\tau\right) = R_{s_as_a}\left(\tau\right) \tag{31}$$

That is to say that the jamming does not introduce any modulation in slow time now.

4.2. The Fast Time Periodic Modulation Jamming

This kind of jamming can be described as follows. For each PRI, the jammer receives the SAR transmitted LFM, modulates the received LFM with a periodic waveform in fast time, and then transmits the modulated LFM back to SAR. This procedure is repeated until the end of a synthetic aperture time. In contrast to the step frequency-shift jamming, this kind of jamming does not introduce any additional modulation in slow time, owing to that the jamming has the same

modulation in fast time during each PRI. Using a similar expression of (10), the periodic modulation with a period of T_{q-r} in fast time can be denoted as

$$q_r(t_r) = q_{0-r}(t_r) \otimes_{t_r} \delta_{T_{q-r}}(t_r) \tag{32}$$

where $q_{0-r}(t) = 0$ for $t_r < -T_{q-r}/2$ or $t_r > T_{q-r}/2$. Multiplying $q_r(t)$ in (32) with $s_r(t_r)$ in (21) ($s_r(t_r t)$ is deemed as the jammer's received LFM in fast time) generates

$$\tilde{s}_{M-r}(t_r) = \left[q_{0-r}(t_r) \otimes_{t_r} \delta_{T_{q-r}}(t_r)\right] \cdot s_r(t_r) \tag{33}$$

Comparing (15) and (33), it can be found that $q_{0-r}(t_r)$, $\delta_{T_{q-r}}(t_r)$ and $s_r(t_r)$ in (33) are the analogies to $q_0(t)$, $\delta_{T_q}(t)$ and $s(t)$ in (15), respectively. According to (17), (18) and (33), $\tilde{s}_{M-r}(t_r)$'s pulse compression can also be written as

$$R_{\tilde{s}_{M-r}s_r}(\tau) = \sum_{m=-\infty}^{+\infty} F_{q-r} Q_{0-r}(mF_{q-r}) \tilde{R}(\tau; T_r, K_r, mF_{q-r}) \tag{34}$$

where $F_{q-r} = T_{q-r}^{-1}$ is the frequency of the modulation waveform $q_r(t_r)$. And

$$Q_{0-r}(mF_{q-r}) = j\mathcal{T}\left\{q_{0-r}(t_r)\right\}\big|_{f_r = mF_{q-r}} \tag{35}$$

Being similar to the analysis of (19) and (20), the interval between the two adjacent peaks is

$$\delta_{\tilde{s}_{M-r}} = F_{q-r}/|K_r| \tag{36}$$

And the maximum value of the mth peak is

$$\Lambda_{\tilde{s}_{M-r}} = F_{q-r} Q_{0-r}(mF_{q-r})(T_r - |mF_{q-r}/K_r|) \tag{37}$$

4.3. The Slow Time Periodic Modulation Jamming

This kind of jamming is similar to the step frequency-shift jamming, in that both of them can cause the effect of insufficient sampling in slow time, except that the former's modulation can be any periodic waveform but not limited to the waveform $u_a(t_a)$ in (25). Also, an instructive comparison can be made between the slow time and fast time periodic modulation jammings, in that they are indeed referred to the same thing mathematically. Here we directly give the corresponding conclusions of the slow time periodic modulation jamming as follows.

If the periodic modulation in slow time is $q_a(t_a)$, F_{q-a} is its period, $F_{q-a} = T_{q-a}^{-1}$ is its frequency, and

$$q_a(t_a) = q_{0-a}(t_a) \otimes_{t_a} \delta_{T_{q-a}}(t_a) \tag{38}$$

The pulse compression result of the slow time periodic modulation jamming is

$$R_{\tilde{s}_{M-a}s_a}(\tau) = \sum_{m=-\infty}^{+\infty} F_{q-a}Q_{0-a}(mF_{q-a})\,\tilde{R}(\tau; T_a, K_a, mF_{q-a}) \quad (39)$$

where,

$$Q_{0-a}(mF_{q-a}) = j\mathcal{T}\{q_{0-a}(t_a)\}\big|_{f_a=mF_{q-a}} \quad (40)$$

The interval between the two adjacent peaks is

$$\delta_{\tilde{s}_{M-a}} = F_{q-a}/|K_a| \quad (41)$$

And the maximum value of the mth peak is

$$\Lambda_{\tilde{s}_{M-a}} = F_{q-a}Q_{0-a}(mF_{q-a})\left(T_{\text{syn}} - |mF_{q-a}/K_a|\right) \quad (42)$$

4.4. The Two-dimensional Periodic Modulation Jamming

Since the signal processings in both the range direction and azimuth direction can be deemed approximately independent from each other after RCMC, the modulations of the jamming in these two directions can also be done independently too, and this kind of jamming is called the two-dimensional periodic modulation jamming. The modulations in fast time and in slow time are similar to the ones discussed in Section 4.2 and 4.3, and we do not repeat them here.

5. EXPERIMENT RESULTS AND ANALYSIS

The jamming experiences were carried out by using a railway SAR system. The parameters of the railway SAR system were listed in Table 1.

Table 1. The main parameters of the railway SAR.

Quantity	Value	Quantity	Value
Carrier frequency	10.48 GHz	Polarization	V V
Pulse width	2 µs	Platform velocity	0.4 m/s
Bandwidth	35 MHz	Equivalent azimuth beamwidth†	3 degrees
Sign of the chirp	positive	Height of the railway	3 m
PRF	40 Hz	Squint angle	0 degree
Peak transmitted power	30 dBm	Sampling rate in fast time	200 MSamples/s

† Both the transmit antenna and the receive antenna are with 40 degrees beamwidth in azimuth direction. A Doppler filter is used to get an equivalent beamwidth of 3 degrees.

The structure of the jammer was shown in Fig. 1. Firstly, the SAR transmitted LFM signal was received and downconverted to the immediate frequency (IF) by the jammer. Then the IF signal was digitized after the analog-to-digital conversion (ADC). The digitized LFM signal was modulated by the fast time waveform and the slow time waveform in sequence, both of which were periodic and were generated by utilizing two lookup tables. For each of the lookup table, only one cycle of the periodic waveform was needed to be included and was read by the modulation control to generate a periodic waveform (as shown in Fig. 1). Finally, the modulate LFM signal was multi-delayed, summed, digital-to-analog converted, upconverted, amplified, and transmitted.

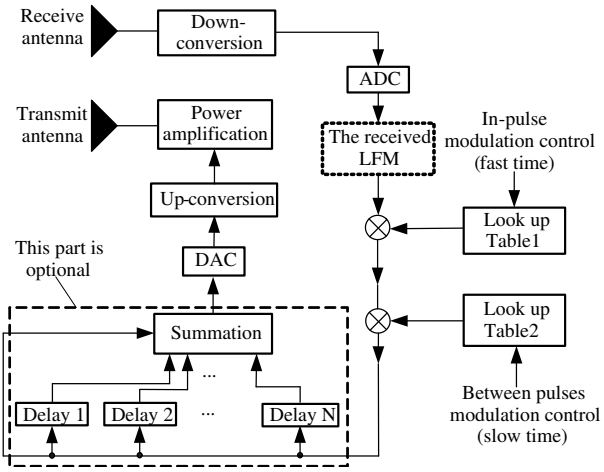

Figure 1. The structure of the DRFM based jammer with periodic modulations.

Two trihedrals, both with the sizes of 20 cm and 30 cm, were put in the imaging scene noted as target A and B (as shown in Fig. 2), both of which were in the azimuth positions of 4.13 m and −2.23 m, and were with approximate 74.25 m and 62.3 m minimum slant ranges away from the railway SAR. The RCSs of both the target A and B are approximate 13.5 dBm^2 and 20.5 dBm^2, since the carrier frequency of the railway SAR is 10.48 GHz. Firstly, a jamming-free image was gotten by the railway SAR (as shown in Fig. 3) for the purpose of comparison with the jammed one. The minimum slant range between the jammer and the railway SAR was approximate 70 m. The azimuth position of the jammer was 1.57 m. Since the chirp rate of the slow time LFM (ST-LFM) is in inverse proportion to the minimum slant range,

the chirp rate changes obviously with the slant range from 70 m to a few hundreds of meters in the imaging scene. Also, the jammings induced by the jammer are often delayed for a few to hundreds of nanoseconds, the chirp rates of their reference ST-LFMs for pulse compression are different from that of the jammer, whereas their ST-LFM chirp rates are essentially equal to that of the jammer. So if a common SAR imaging algorithm, e.g., range Doppler (RD), chirp scaling (CS), is used, then the jammings will be defocused. This phenomenon is less obvious in an airborne or spaceborne SAR, because the ST-LFM chirp rate does not change obviously between different slant ranges. In order to analyze the properties of the jammings, the common SAR imaging algorithms were not used in our experiences. Instead, an imaging algorithm with a fixed ST-LFM chirp rate of 0.152 Hz/s (the chirp rate of the jammer) was used. The minimum slant ranges of the two trihedrals were approximate to that of the jammer, so their ST-LFM chirp rates did not show much differences from each other. However,

Figure 2. The imaging scene.

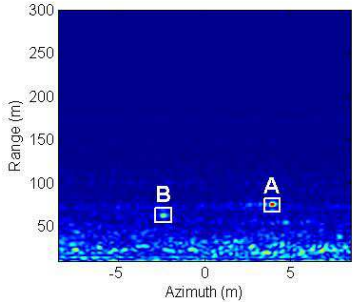

Figure 3. SAR imaging in a jamming-free environment.

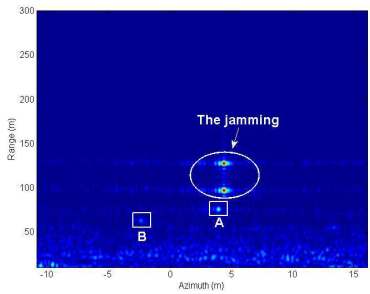

Figure 4. Fixed frequency-shift jamming.

the two trihedrals were still somewhat defocused in azimuth direction, due to the instable movement of the railway SAR. For other parts of the imaging scene, they were obviously defocused, because their ST-LFM chirp rates were different from that of the jammer. The results of the jamming experiences were shown as follows.

① The single tone modulated jamming

According to (8), there are two isolated peaks in this kind of jamming. The absolute value of the tone frequency of the jamming was 1.75 MHz in our experiment, corresponding to a theoretical 30 m interval between the two peaks which was in good accordance with the experiment result (As shown in Fig. 4).

② The step frequency-shift jamming

In our experiment, a single tone modulation was used instead of the complex tone modulation to generate the step frequency-shift jamming, and the initial frequency of the single tone was 1.75 MHz. In this case, the imaging result of jamming were divided into two parts with a gap of 30 m width in the range direction (as shown in Fig. 5). The tone frequency did not changes from pulse to pulse, but changed one time per two pulses with a step of 1.75 MHz. So the interval between two adjacent peaks in range direction is 15 m. The frequency of the slow time modulation caused by the step frequency-shift in fast time is 2 Hz, i.e., the tone frequency in fast time will return to its initial value after every 20 pulses since the PRF is 40 Hz. According to (28), the interval between the two adjacent peaks in azimuth direction is 5.25 m in theory which is somewhat different from the result of 5 m in our experiment. And this may be due to the inaccuracy of the jammer's modulation in fast time.

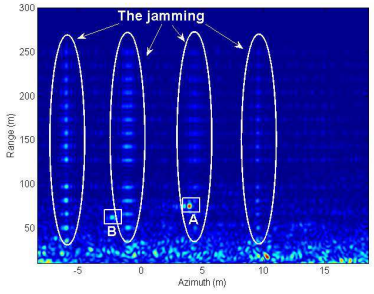

Figure 5. Step frequency-shift jamming.

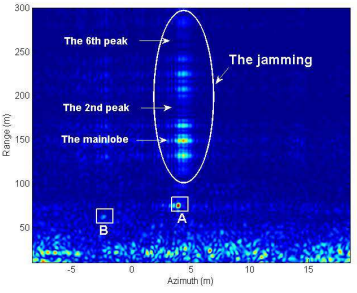

Figure 6. The jamming with periodic modulation in fast time.

③ The fast time periodic modulation jamming

In our experiment, the $q_{0-r}(t_r)$ in (32) was set as

$$\begin{aligned} q_{0-r}(t_r) &= \text{rect}\left[\frac{t_r + 5T_{q-r}/8}{T_{q-r}/8}\right] + \text{rect}\left[\frac{t_r + 3T_{q-r}/8}{T_{q-r}/8}\right] \\ &\quad + \text{rect}\left[\frac{t_r - 3T_{q-r}/8}{T_{q-r}/8}\right] + \text{rect}\left[\frac{t_r - 5T_{q-r}/8}{T_{q-r}/8}\right] \end{aligned} \quad (43)$$

And $q_{0-r}(t_r)$'s Fourier transform is

$$\begin{aligned} Q_{0-r}(f_r) &= 2\frac{\sin(\pi f_r T_{q-r}/8)}{\pi f_r} \\ &\quad [\cos(3\pi f_r T_{q-r}/4) + \cos(5\pi f_r T_{q-r}/4)] \end{aligned} \quad (44)$$

In this case, (35) can be written as

$$\begin{aligned} Q_{0-r}(mF_{q-r}) &= 2\frac{\sin(\pi f_r T_{q-r}/8)}{\pi f_r}[\cos(3\pi f_r T_{q-r}/4) \\ &\quad + \cos(5\pi f_r T_{q-r}/4)]\big|_{f_r = mF_{q-r}} \\ &= 2\frac{\sin(\pi m/8)}{\pi m F_{q-r}}[\cos(3\pi m/4) + \cos(5\pi m/4)] \end{aligned} \quad (45)$$

Notice that, when $m = \pm 2, \pm 6$, it has $Q_{0-r}(mF_{q-r}) = 0$, so the value of the 2nd and the 6th peaks are zeros (As shown in Fig. 6). Also the jamming's modulation frequency is 2 MHz in fast time, corresponding to a theoretical interval of 17.1 m between two adjacent peaks in range direction.

④ The slow time periodic modulation jamming

The jamming's slow time modulation frequency is 0.3 Hz, corresponding to a theoretical interval of 0.787 m between the two adjacent peaks in the azimuth direction which is somewhat different from the result of 0.75 m in our experiment (as shown in Fig. 7). And this may also be due to the inaccuracy of the jammer's modulation in slow time.

⑤ The two-dimensional periodic modulation jamming

Here the jamming used the same form of fast time modulation as discussed in ③. Notice that the 2nd and the 6th peaks in the range direction are also zeros (as shown in Fig. 8). The slow time modulation frequency is 0.6 Hz, corresponding to a theoretical interval of 1.57 m in the azimuth direction, which is somewhat different from the result of 1.5 m in our experiment. As can be seen from Fig. 8, the jamming's modulations in both the range and azimuth directions can be deemed to be independent to each other.

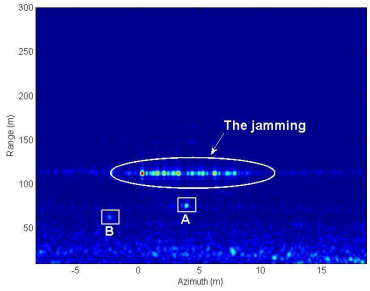

Figure 7. The jamming with periodic modulation in slow time.

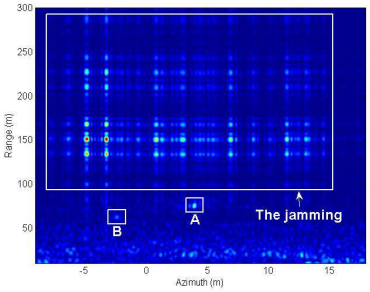

Figure 8. The jamming with periodic modulations in both of the two directions.

6. CONCLUSION

A coherent jammer was developed by using the periodic modulation technology in this paper. In contrast to other jammers using the coherent jamming, this kind of jammer does not need to estimate the slow time parameters of SAR's transmitted signal in high precision. It only needs to use an off-the-shelf DRFM structure to achieve a good coherency with the SAR's transmitted signal and to modulate its received SAR signal with the periodical waveforms both in the fast and slow time to induce bright and isolated points in the SAR image. Thus the structure of this kind of jammer is simple and easy to be designed. Most importantly, its transmitted power is much lower than that of a noise jammer which makes our jammer more suitable to work in a SAR ECCM environment.

REFERENCES

1. Zhao, Y. W., M. Zhang, and H. Chen, "An efficient ocean SAR raw signal simulation by employing fast Fourier transform," *Journal of Electromagnetic Waves and Applications*, Vol. 24, No. 16, 2273–2284, 2010.
2. Chan, Y. K. and V. C. Koo, "An introduction to synthetic aperture radar (SAR)," *Progress In Electromagnetics Research B*, Vol. 2, 27–60, 2008.
3. Chan, Y. K. and S. Y. Lim, "Synthetic aperture radar (SAR) signal generation," *Progress In Electromagnetics Research B*, Vol. 1, 269–290, 2008.

4. Narayanan, R. M., M. C. Shastry, P.-H. Chen, and M. Levi, "Through-the-wall detection of stationary human targets using doppler radar," *Progress In Electromagnetics Research B*, Vol. 20, 147–166, 2010.
5. Condley, C. J., "Some system considerations for electronic countermeasures to synthetic aperture radar," *IEE Colloquium on Electronic Warfare Systems*, Her Majesty's Stationery Office, London, 1990.
6. Dumper, K., P. S. Cooper, A. F. Wons, C. J. Condley, and P. Tully, "Spaceborne synthetic aperture radar and noise jamming," *Proc. IEE Radar*, 411–414, 1997.
7. Wu, X., D. Dai, and X. Wang, "Study on SAR jamming measures," *IET International Conference on Radar Systems*, 176–179, Edinburgh, England, 2007.
8. Wu, X, D. Dai, X. Wang, and H. Lu, "Evaluation of SAR jamming performance," *2007 International Symposium on Microwave, Antenna, Propagation and EMC Technologies for Wireless Communications*, 1476–1479, 2007.
9. Dai, D., X. Wu, X. Wang, and S. Xiao, "SAR active-decoys jamming based on DRFM," *IET International Conference on Radar Systems*, 1–4, 2007.
10. Thayaparan, T. and C. Wernik, "Noise radar technology basics," *Defence R&D Canada-Ottawa*, 2006.
11. Qiao, S., Z.-G. Shi, T. Jiang, and L.-X. Ran, "A new architecture of UWB radar utilizing microwave chaotic signals and chaos synchronization," *Progress In Electromagnetics Research*, Vol. 75, 225–237, 2007.
12. Jiang, T., J. Long, Z. Wang, S. Qiao, W. Cui, W. Ma, J. Huangfu, and L. Ran, "Experimental investigation of a direct chaotic signal radar with colpitts oscillator," *Journal of Electromagnetic Waves and Applications*, Vol. 24, No. 9, 1229–1239, 2010.
13. Xu. X. and R. M. Narayanan, "FOPEN SAR imaging using UWB step-frequency and random noise waveforms," *IEEE Trans. on AES*, Vol. 37, No. 4, 1287–1300, 2001.
14. Garmatyuk, D. S. and R. M. N., "ECCM capabilities of an ultrawideband bandlimited random noise imaging radar," *IEEE Trans. on AES*, Vol. 38, No. 4, 1243–1255, 2002.
15. Klemm, R., *Principles of Space-time Adaptive Processing*, The Institution of Engineering and Technology, London, United Kingdom, 2002.
16. Mrstik, V., "Agile-beam synthetic aperture radar opportunities,"

IEEE Trans. on AES, Vol. 34, No. 2, 500–507, 1998.

17. Ender, J. H. G., P. Berens, A. R. Brenner, L. Rossing, and U. Skupin, "Multi channel SAR/MTI system development at FGAN: From AER to PAMIR," *2002 IEEE International Geoscience and Remote Sensing Symposium*, Vol. 3, 1697–1701, 2002.
18. Willis, N. J., *Bistatic Radar*, SciTech Publishing Inc. Raleigh, NC, USA, 2005.
19. Rodriguez-Cassola, M., S. V. Baumgartner, G. Krieger, and A. Moreira, "Bistatic TerraSAR-X/F-SAR spaceborne-airborne SAR experiment: Description, data processing, and results," *IEEE Trans. on AES*, Vol. 48, No. 2, 781–794, 2010.
20. Paine, A. S., "An adaptive beamforming technique for countering synthetic aperture radar (SAR) jamming threats," *2007 IEEE Radar Conf.*, 630–634, 2007.
21. Cumming, I. G. and F. H. Wong, *Digital Processing of Synthetic Aperture Radar Data*, Artech House, 2004.